PEER-REVIEWED ARTICLE bioresources.com

New Method to Evaluate the Frictional Behavior within the Forming Gap during the Deep Drawing Process of Paperboard

Alexander Lenske,* Tobias Müller, Marek Hauptmann, and Jens-Peter Majschak

To evaluate the influence of different normal forces and contact temperatures on the frictional behavior of paperboard during the deep drawing process, a new measurement punch was developed to measure the normal force, which induced the friction within the gap between the forming cavity and punch. The resulting dynamic coefficient of friction was calculated and reproduced *via* a new developed substitute test for the friction measurement device, which was first introduced in Lenske *et al.* (2017). The normal force within the forming gap during the deep drawing process was influenced by the blankholder force profile, the contact temperature, and the fiber direction. The friction measurements with the substitute test showed a strong dependency between the applied normal force and the dynamic coefficient of friction. Furthermore the frictional behavior was influenced by the contact temperature and the wrinkle formation.

Keywords: Friction behavior; Friction measurement; Paperboard; Tribocharging; Contact electrification; Triboelectrification; Deep drawing process; 3D-forming

Contact information: Department of Processing Machines and Processing Technology, Technische Universität Dresden, Bergstrasse 120, 01069 Dresden, Germany;
** Corresponding author: alexander.lenske@tu-dresden.de*

INTRODUCTION

During the deep drawing process with immediate compression, paperboard is drawn by a punch into a cavity against the resistance induced through a blank holder (Scherer 1932). A few millimeters after passing the forming cavity infeed radius, inevitable wrinkles occur due to the excess material that is immediately compressed between the punch and the forming cavity. Using a hydraulic system for a permanent force control of the blank holder and heated tools, Hauptmann and Majschak (2011) showed that the blank holder force and temperature sum of the tool-set are major factors that influence the distribution of the characteristic wrinkles and consequently the quality of the deep drawing process. The wrinkle distribution can be directly related to modes of failure, such as ruptures, discoloration, or earing formations of the wall section. Such failures interfere with the quality of the formed parts significantly and correlate with the dynamic friction between the paperboard and the surface of the tool set, especially within the gap between punch and forming cavity (Hauptmann 2010). The frictional force within the forming gap is induced through a compression or normal force, which depends on the interaction between local material accumulation within each wrinkle and the geometric shape of the forming gap. The gap size is designed based on empirical values (Tenzer 1989) testing different forming parameters with different gap sizes using several punches with different diameters and cone angles. Currently, neither the gap force nor the resulting dynamic coefficient of friction

within the forming gap was measured during the deep drawing process with immediate compression comparing different parameters against each other. Tanninen *et al.* (2017) described a novel technique to measure the punch force during press forming using four miniature column load cells. They calculated the resulting dynamic coefficient of friction for the area between the blank holder and the female mould cavity, but this approach is unfit for the requirements of the deep drawing process with immediate compression.

The purpose of this paper is to extend the work presented by Lenske *et al.* (2017), to evaluate the influence of different normal forces and contact temperatures on the friction behavior within the forming gap during the deep drawing process. Therefore, a newly developed method is introduced to determine the normal force within the gap between the forming cavity and punch during the deep drawing process. With this gap force and the previous measured punch force (Hauptmann 2010), the resulting dynamic coefficient of friction can be calculated. The second part of this paper is to reproduce the results of the friction behavior during the deep drawing process with a newly developed substitute test, based on the friction measurement device, which was introduced by Lenske *et al.* (2017). Finally, both dynamic coefficients of friction that were calculated from the deep drawing process and the substitute test are compared to each other, and the results are evaluated.

EXPERIMENTAL

Materials

In the following experiments, the commercially available material called Trayforma Natura (Stora Enso, Imatra, Finland) was used, which consisted of three layers of virgin-quality fiber, with a grammage of 350 g/m^2, and a thickness of 0.43 mm to 0.45 mm. The middle layer also contains chemithermomechanical pulp (CTMP), which has a higher lignin content and is therefore very stiff. The tensile strength was in accordance with DIN EN ISO 1924-2 (2009), and was 22 N/mm in the machine direction (MD), 11.5 N/mm in the cross-direction (CD), and under standard climate conditions (23 °C; 50% relative humidity). The moisture was 7.9% ± 0.4% in accordance with the EN ISO 287 (2009) standard.

Methods

3-D forming equipment/measurement-punch

The 3-D forming of the paperboard blanks was conducted with a servo-hydraulic press, built at TU Dresden and introduced by Hauptmann in 2010 (Hauptmann 2010). The force control of the blank holder used a grid point system allowing programmable blank holder force profiles for 10 grid points that referred to the drawing depth of the part that was formed. For the experiments and the following discussion, two different blank holder force profiles were used. During the first profile, the blank holder force decreased linearly in relation to 25 mm of forming depth from 3200 N at the beginning of the process to 500 N when the paperboard was fully drawn into the forming gap. These decreasing blank holder force profile was also used in Lenske *et al.* (2017), meaning a constant pressure of 0.3 MPa. The second profile of the blank holder force was held constant at 500 N. The tools, including punch, forming cavity, and blank holder, were equally heated with three different temperatures at 23 °C, 60 °C, and 120 °C. The forming cavity and the blank holder were composed of polished stainless steel (Material No. X5CrNi18-10 or 1.4301 in accordance with the DIN EN 10027-2 (2015) standard).

To examine the normal force within the forming gap and coefficient of friction during the deep drawing process, a new developed measuring-punch was used (Fig. 1). The geometric form and data corresponds to the punch used in Lenske *et al.* (2017) and is shown in Table 1. Inside the frame of the measurement punch, one S-type force sensor was used (KD9363s; ME Messsysteme, Hennigsdorf, Germany) with a measuring range of 10 kN and accuracy class of 0.1% that receives the normal force induced through the paperboard within the deep drawing process through a pressure plate. To avoid damages of the wall section of the formed part and to measure the correct normal force, the pressure plate must be flush with the surface of the punch-frame. The pressure plate was connected with permanent magnets inside two mounting plates with the force senor and the punch-frame. The measuring-punch consisted of stainless steel (X5CrNi18-10 or 1.4301 in accordance with the DIN EN 10027-2 (2015) standard).

Hauptmann and Majschak (2011) described the influence of the blank holder force and the contact temperature on the wrinkle formation of the wall section of the formed parts. The wrinkle formation must also have an influence on the material thickness at the edge of the wall section of the deep drawn parts and therefore on the normal force within the forming gap. To demonstrate this effect, the material thickness was measured down to a hundredth of a millimeter with a caliper (Mitutoyo Absolute Digimatic, Neuss, Germany), which was equipped with a digital display.

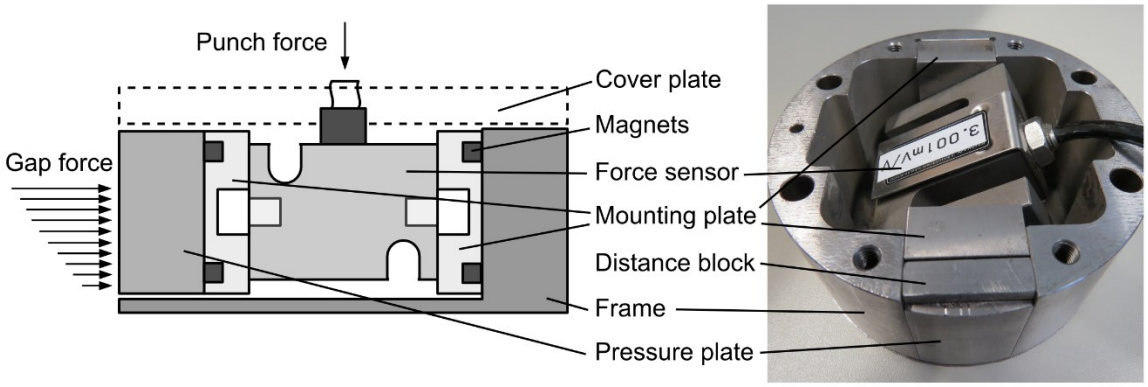

Fig. 1. Schematic tool-setup of the measurement punch and constructive implementation

Table 1. Geometrical Data and Parameters of the Deep Drawing Process

Sample Base Diameter	110 mm
Drawing Depth	25 mm
Cone Angle of the Punch	0.5°
Infeed Radius	2 mm
Drawing Clearance	0.35 mm
Blank Holder Profiles	3200 N to 500 N; 500 N to 500 N
Relative Velocity (Punch)	20 mm/s
Temperature (Tool-set)	23 °C; 60 °C; 120 °C
Relative Humidity	50% RH

Friction tester and strip-testing

The friction tests were conducted using the friction tester that was presented in Lenske *et al.* (2017), using the new developed double-strip testing method, as shown in Fig. 2. These tests were performed to simulate the friction behavior within the forming gap between the forming cavity and punch during the deep drawing process. A paperboard

sample is prepared with two creasing lines and folded along these lines around a rectangular specimen holder, which represents the punch in this substitute test. The specimen holder is mounted within a lever system and could be separately heated. To guarantee a parallel motion of the specimen holder in relation to the tool sample surface, the specimen holder is pivoted on the first attachment and loosely mounted on the second attachment using a M6 through-hole and a M5 screw. The paperboard sample is held in place on the front of the specimen holder with a small permanent magnet. For the friction measurement process, the double-strip was clamped between both exchangeable tool samples with four different normal loads at 150 N, 400 N, 800 N, and 1200 N, and afterwards removed from the tool-set at 20 mm/s relative velocity. During the pulling sequence, the measured force at the lower tool represents the friction force between the paperboard and the metal surface, which is evaluated in the following analysis. The contact pressure analysis and calibration of the tool-set in terms of parallelism to the paperboard sample was completed just like in Lenske *et al.* (2017). The tools used for the friction measurement process were composed of polished stainless steel (X5CrNi18-10 or 1.4301 in accordance with the DIN EN 10027-2 (2015) standard) and were both separately ground on the side of the tool bulk.

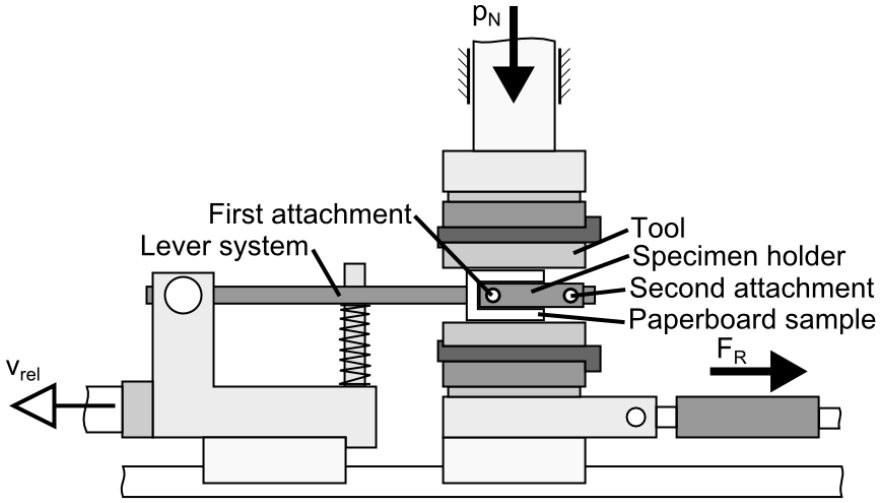

Fig. 2. Double-strip testing method schematic

Test procedure

To ensure that there was no contamination of the paper samples, clean surgical gloves were worn, and the metal tools for the deep drawing process and friction measurement process were cleaned before each test series with a sterile cotton wipe (Dastex series 100; Dastex Reinraumzubehör GmbH, Muggensturm, Germany) soaked with acetone. All of the repetitions of one test series with the same parameter setup were performed using fresh paperboard samples for each repetition, without further cleaning or discharging in-between. Each test series of the deep drawing process was performed with 70 repetitions in a row. Because a lesser amount of paperboard is needed, the friction measurement with the double strip testing method was performed with 100 repetitions in a row.

RESULTS AND DISCUSSION

Deep Drawing Process

The influence of three different contact temperatures on the punch force profile is shown in Fig. 3 for two blank holder force profiles a) with 3200 N to 500 N and b) with 500 N to 500 N at 20 mm/s punch velocity. The punch force profiles with unheated tools at 23 °C, inclined rapidly to a peak force at 25 mm punch position where the paperboard left the contact of the blank holder and simultaneously was completely drawn into the forming cavity (marked by the dashed line in Fig. 3). At 50 mm punch position the paperboard sample left the forming cavity. Between both positions, the punch force consists only of the friction force between the forming cavity and paperboard (Hauptmann 2010).

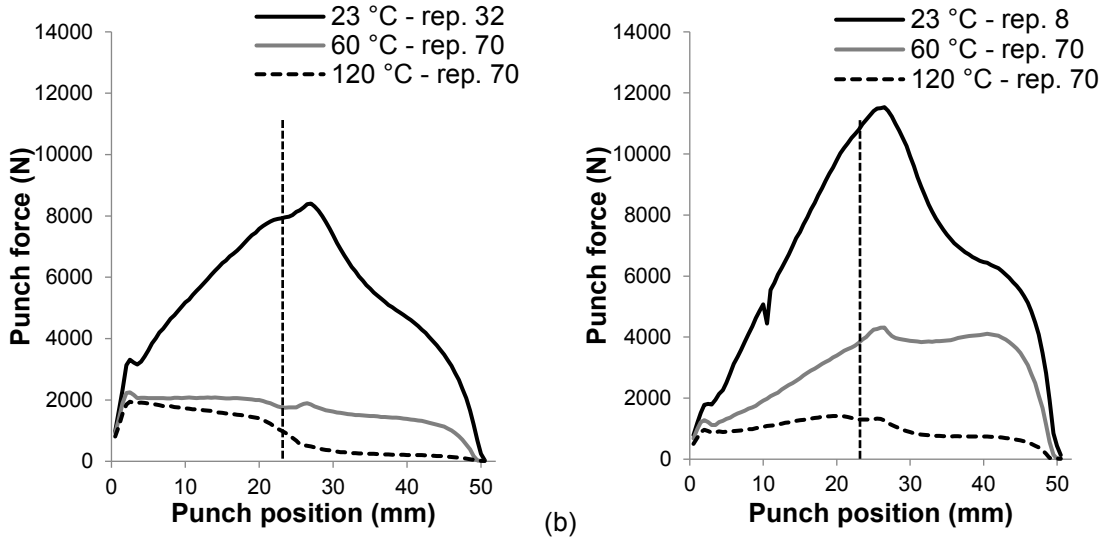

Fig. 3. Punch force profiles for the last repetition in every test series for 23 °C, 60 °C, and 120 °C; a) 3200 N to 500 N blank holder force profile, and b) 500 N to 500 N blank holder force profile

After succeeding repetitions of the deep drawing process, the punch force profiles increased noticeably over the complete punch movement for both of the blank holder force profiles similar to the results in Lenske *et al.* (2017). To evaluate the progression of the triboelectric charging due to the frictional contact between the tools and the paperboard sample for the deep drawing process, the progression rate was calculated in Eq. 1,

$$Progression\ rate_{\mathrm{n}} = \left(\frac{100 \cdot F_{\mathrm{Punch,rep.n}}}{F_{\mathrm{Punch,rep.1}}}\right) - 100 \quad (1)$$

relating the punch force ($F_{\mathrm{Punch,rep.n}}$) of one of the n succeeding repetitions to the punch force ($F_{\mathrm{Punch,rep.1}}$) of the first repetition (Fig. 4).

In contrast to the results in Lenske *et al.* (2017), the test series with 3200 N to 500 N blank holder force profile and unheated tools ended after 32 repetitions in a row of undamaged forming parts. After that, all following repetitions of the deep drawing process failed due to rupture of the wall section shortly before the paperboard left the contact between blank holder and forming cavity. These failures indicated an increased triboelectric charging and an increased friction force between the paperboard, the tool surfaces of the forming cavity, and the blank holder. Between the test series with the

standard punch in Lenske *et al.* (2017) and the test series with the measurement punch depicted in Fig. 3, three months passed. During this time period, 500 repetitions with different parameter setups of the deep drawing process were performed using the same tool set every time. To guarantee the same test conditions before every test series, the tool surface was cleaned or discharged through contact with an acetone-soaked cotton wipe (Lenske *et al.* 2017). Lowell (1988) showed that charge transfer is influenced by the contacting sample history every time. The charge transfer increases with repeated contact-and-discharge cycles for metal and insulator combinations, and the increase becomes less rapid as the cycle continues (Lowell 1988). Thus, with the progression of test series for the deep drawing process with the same tool-set over 3 months, the charge transfer between the paperboard and tool surface must have increased. While the charge transfer correlates with the coefficient of friction (Burgo *et al.* 2013), the constant limit for the friction force must have increased too, and therefore it reached the breaking strength of the paperboard. In contrast, the test series in Lenske *et al.* (2017) consisted of only 40 repetitions without failure, not many more than the 32 repetitions used in this paper. Taking the Lowell (1988) theory into account, with increasing the overall repetitions using the same tool-set every time, the speed of the tribocharging increased, reaching the same charging level within lower numbers of repetitions. However, future evaluations should use more repetitions to be sure that a constant charging state is reached without failure due to rupture. With heated tools, the test series could be performed for 70 repetitions in a row without failure for both blank holder force profiles. The progression rate was depicted with only a few points of the standard deviation for better clarity, but showed nonetheless that the deep drawing system reached a constant state, similar to the results in Lenske *et al.* (2017).

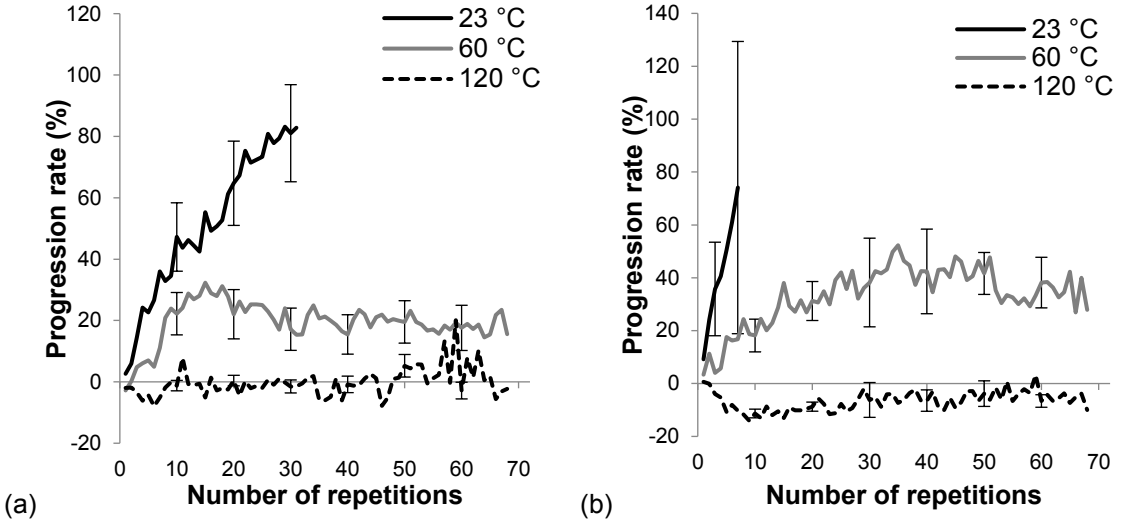

Fig. 4. Progression rates of the punch force profiles for different numbers of repetitions for 23 °C, 60 °C, and 120 °C; a) with 3200 N to 500 N blank holder force profile, and b) with 500 N to 500 N blank holder force profile

The corresponding gap forces calculated as an average after several repetitions in MD and CD for both blank holder force profiles and all tool temperatures are shown in Fig. 5. Generally, the gap force began to rise after 5 mm drawing depth. Obviously there is no or only a slight material accumulation in this area of the drawing wall and consequently no detectable compression force compared to the gap width between the forming cavity and

punch. Müller *et al.* (2017a) described a method to evaluate the wrinkle distribution over the drawing height recording the sample surface topography through laser-distance measurement. Müller *et al.* (2017a) excluded the first 4 mm of the drawing height from the studies, because no wrinkles formed in this section of the wall or the wrinkles are too fine to be detectable. The gap force in Fig. 5 increased until the entire material was drawn into the forming gap after roughly 25 mm. Scherer (1932) used a blank holder made of glass to evaluate the occurrence of wrinkles, and observed that the number of wrinkles in the wall section of the drawn geometry depends on the forming height. Müller *et al.* (2017b) showed the same correlation using the laser distance measurement method described in Müller *et al.* (2017a). With increasing forming height, the increasing material excess accumulates in these wrinkles and due to the incompressible forming gap, the compression force within the gap must also increase. After the peak, the gap force declined. This phenomenon may have been related to stress relaxation mechanics. When paperboard is charged with a constant load a decrease of the stress response can be observed over time (Niskanen 1998). In contrast, shortly before the drawing wall left the forming cavity, there was a slight incline of the gap force, which could have been related to the manufacturing process of the tool surface. After the machining of the forming cavity the tool surface was polished by hand with a polishing paste. Typically, the amount of surface material that was removed during this process was not homogenous at every point of the surface. Therefore, the width of the forming gap differed over the punch movement, resulting in an inconsistent compression force. After leaving the forming cavity the gap force decreased to zero.

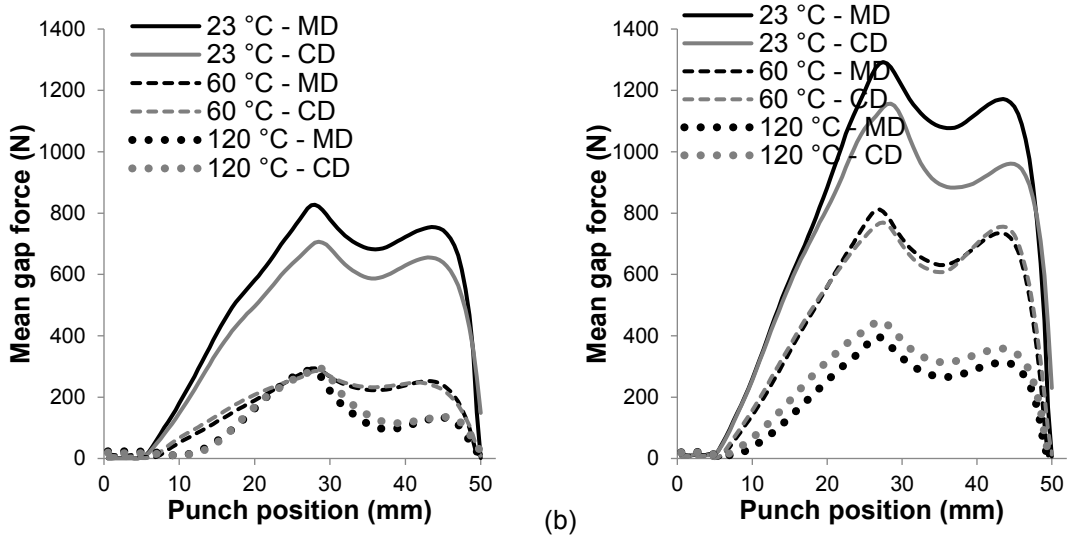

Fig. 5. Mean values of the gap force in MD and CD for 23 °C, 60 °C, and 120 °C; a) with 3200 N to 500 N blank holder force profile and b) with 500 N to 500 N blank holder force profile

For unheated tools at 23 °C the mean gap force profile in the machine direction was noticeably higher than in the cross-machine direction. Paperboard has an anisotropic fiber orientation, due to the papermaking process where more fibers are aligned in machine direction than perpendicularly (Niskanen 1998). Steenberg (1947) described the relation between the breaking strength, breaking elongation, and the anisotropic fiber orientation for tensile tests. The breaking strength increases in machine direction and decreases in cross-machine direction. The breaking elongation is conducted in a reverse manner. When the resistance against the external load perpendicular to MD is significantly lower than in

CD, the material accumulation must be higher in MD than in CD (Hauptmann 2017). With a higher material accumulation in MD, the gap force must be higher than in CD due to the incompressible forming gap. Furthermore, the probable inhomogeneous surface of the forming cavity in the drawing direction could not be responsible for the difference between MD and CD, because the gap force measurements were performed on the same spot of the forming cavity every time. Generally, the constant 500 N blank holder force profile induced a noticeably higher punch force and gap force profile than the test series with the 3200 N to 500 N blank holder force profile. A lower blank holder force at the beginning of the deep drawing process induces a lower amount of wrinkles (Hauptmann *et al.* 2016), resulting in higher material accumulations in every wrinkle and consequently there is a higher compression force within the forming gap. Müller *et al.* (2017b) examined the relation between the blank holder force and wrinkle quantity and concluded that higher blank holder forces induce a fine and evenly distributed wrinkle arrangement. The incline of the progression rate for the test series with a constant 500 N blank holder force and unheated tools was remarkably steeper, which indicated that the triboelectric charging and resulting friction force were force dependent. According to the increasing load, the paperboard samples ruptured after only 8 repetitions. To gain at least 8 repetitions for both fiber directions between the test series in MD and CD, the tool surfaces were discharged with an acetone-soaked cotton wipe.

The mean gap force profiles and punch force profiles decreased noticeably with increased contact temperature and higher blank holder force at the beginning of the deep drawing process. Hauptmann and Majschak (2011) described similar effects and observed decreasing wrinkle distances with increasing contact temperature and blank holder force. Müller *et al.* (2017b) shows that a high temperature of the forming cavity improves the wrinkle distribution towards more evenly distributed wrinkle arrangements. Figure 6 shows 12 samples of the wall section of deep drawn parts for different forming parameters and fiber directions, as expressed in Table 2.

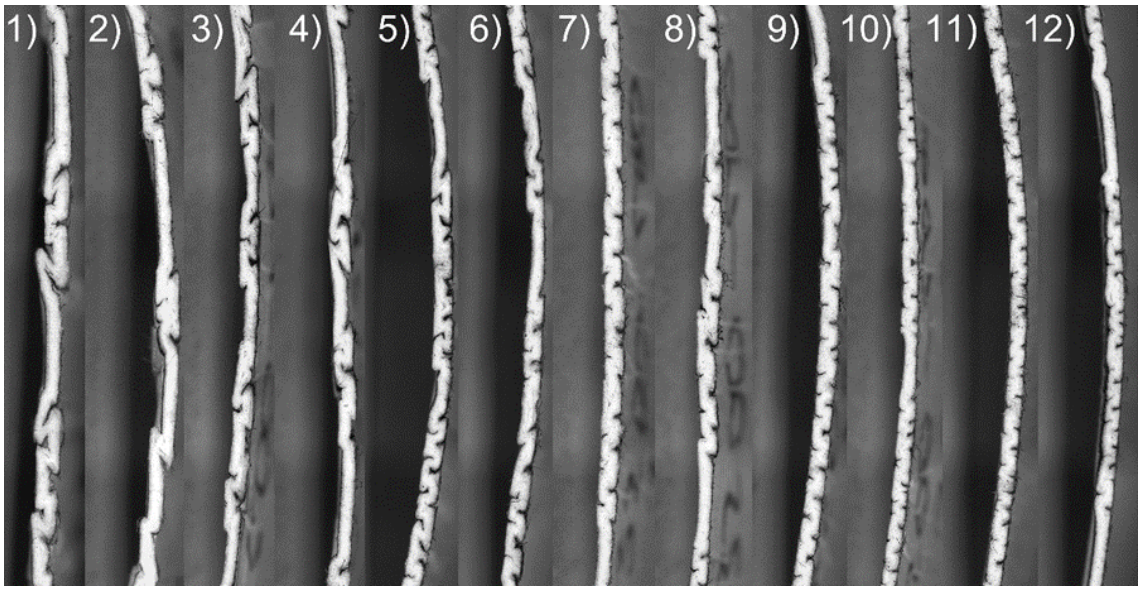

Fig. 6. Samples of the wall section of deep drawn parts for different forming parameters and fiber directions

Table 2. Influence of Wrinkle Formation at Material Thickness

	500 N to 500 N; 23 °C	500 N to 500 N; 60 °C	500 N to 500 N; 120 °C	3200 N to 500 N; 23 °C	3200 N to 500 N; 60 °C	3200 N to 500 N; 120 °C
MD	1) 0.57 mm	3) 0.53 mm	5) 0.52 mm	7) 0.53 mm	9) 0.51 mm	11) 0.50 mm
CD	2) 0.52 mm	4) 0.53 mm	6) 0.56 mm	8) 0.50 mm	10) 0.50 mm	12) 0.49 mm

A better wrinkle distribution caused more uniform material accumulation within the wrinkles and therefore a decreased compression force within the incompressible drawing gap between the punch and forming cavity. Furthermore, with increasing temperature and high blank holder force the initial wrinkle height, referring to as drawing height when first wrinkles appear or are detectable (Hauptmann *et al.* 2015), must be increased because the mean gap force for heated tools inclined noticeably later than with unheated tools. This effect was not be observed for the test series with the low blank holder force profile, likely because the temperature and blank holder force enhanced the initial wrinkle height. The difference between the mean gap force profiles in MD and CD for the high blank holder force profile disappeared completely with increasing temperature and with the lower blank holder force profile for 60 °C. Müller *et al.* (2017b) stated that the wrinkle quantity did not vary much between MD and CD with higher contact temperatures. In contrast, with 120 °C and a low blank holder force profile the mean gap force in CD was higher than in MD. These effects could be demonstrated by measuring the influence of the wrinkle formation on the material thickness at the edge of the wall section of the deep drawn parts. The values in Table 2 are the average thickness of 4 samples for every parameter setup, which were cut out of the wall section at a length of 30 mm. The corresponding pictures of the wall sections are depicted in Fig. 6. With a low blank holder force and unheated tools the thickness in the MD was higher than in CD, which resulted in a higher gap force in MD. With increased temperature at 60 °C, the material thickness for both fiber directions aligned and with 120 °C the material thickness in CD was higher than in MD, confirming the results in Fig. 5 for the low blank holder force profile. The material thickness for the high blank holder force profile and three different tool temperatures also reflected the results of the gap forces in Fig. 5.

To evaluate the friction behavior during the deep drawing process within the forming gap, the dynamic coefficient of friction between forming cavity and paperboard ($\mu_{\text{forming gap}}$) in relation to the punch position was calculated according to Eq. 2,

$$\mu_{\text{forming gap}} = \frac{1}{12} \cdot \frac{F_{\text{Punch,rep.n}}}{\sum F_{Gap}/_{n}} \quad (2)$$

relating the punch force ($F_{\text{Punch,rep.n}}$) of one of the n succeeding repetitions to the average of the normal force within the forming gap (F_{Gap}) for all repetitions of one test series.

The dynamic coefficient of friction was calculated as an average of all repetitions in the MD and CD in relation to the current punch position, due to the difference in both fiber directions especially for unheated tools. The opening angle of the pressure plate (Fig. 1) was designed for 30°. Furthermore, only the last 25 mm of the forming process were evaluated, because only then the punch force consisted of the friction force between the forming cavity and paperboard alone. Figure 7a shows the dynamic coefficients of friction for the deep drawing test series for both blank holder force profiles and all three tool temperatures. Figure 7b shows all mean values of the dynamic coefficient of friction, as an average of all measuring points for one repetition, for all repetitions of the respective test

series. Both dynamic coefficients of friction for unheated tools decreased with an increase in the punch position and ended after a couple of repetitions due to rupture. The progression of the mean values of the dynamic coefficient of friction indicated that the dynamic coefficient of friction could increase furthermore. In contrast to this, the dynamic coefficients of friction for all test series with heated tools reached a constant charging state. Generally, when increasing the temperature, the dynamic coefficient of friction decreased noticeably, similar to the results in Lenske *et al.* (2017). There was no significant influence of the normal force for heated tools on the coefficients of friction. Furthermore, the influence of the normal force within the forming gap for unheated tools could not observed due to rupture of the deep drawn samples after 8 or 32 repetitions.

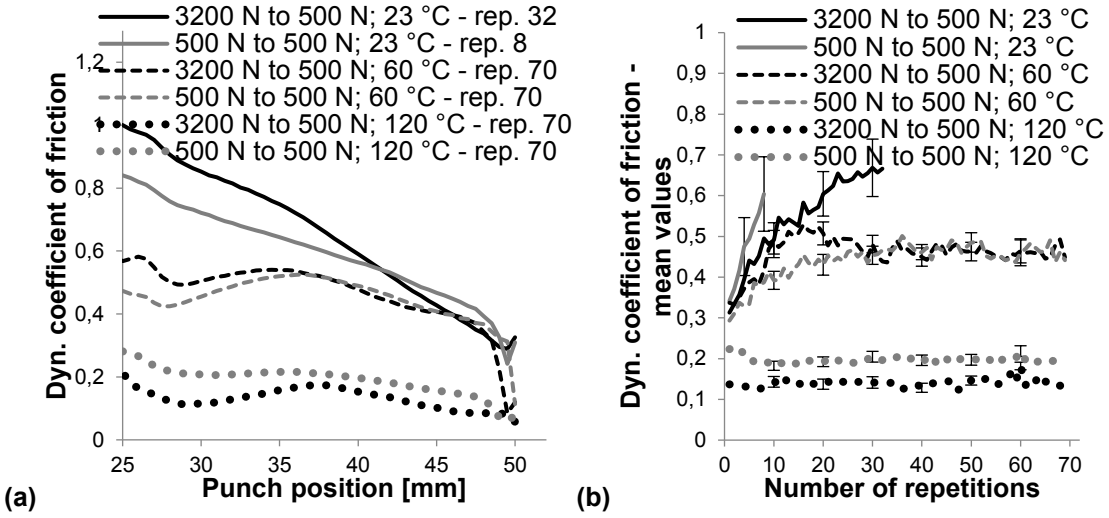

Fig. 7. a) Influence of the blank holder profiles and tool temperature on the dynamic coefficient of friction during the deep drawing process, b) mean values of the dynamic coefficients of friction for different numbers of repetitions

Friction Measurement and Evaluation

To simulate the friction behavior in the drawing gap between the punch and forming cavity, the double-strip testing method was performed with the parameters measured during the deep drawing process. To simplify the test procedure and maintain the comparability with further test series, the highest values of the gap force profiles were used as constant normal force for the friction measurement, as shown in Fig. 5. During the deep drawing process there was a constant frictional contact between the paperboard and forming cavity for a sliding distance of about 50 mm including the area under the blank holder and within the drawing gap. In contrast, the friction contact between the forming cavity and the paperboard sample within the forming gap only lasted 25 mm, when the paperboard was completely drawn into the forming gap. Furthermore, the fiber orientation of the paperboard had a noticeably influence on the compression force within the forming gap during the deep drawing process, at least for the unheated tools. Figure 8, a) shows the dynamic coefficients of friction for 800 N constant normal force, 20 mm/s relative velocity, and unheated tools at 23 °C for a sliding distance of 30 mm and 55 mm. The paperboard samples for the two test series were cut out in cross-machine direction and for one test series in machine direction. To describe the progression rate of the dynamic coefficient of friction resulting from the triboelectric charging, the average value of the dynamic coefficient of friction for all measuring points in one repetition over the sliding distance

was calculated according to Eq. 3 and is shown in Fig. 8, b),

$$\mu_{\text{mean value}} = \frac{\sum \mu_{\text{i}}}{n} \quad (3)$$

The standard deviation, which described the non-linear progression of the dynamic coefficient of friction in Fig. 8a in relation to the sliding distance, is depicted in Fig. 8b only in a few points for better clarity. There was no difference between both fiber directions for the dynamic coefficient of friction after 100 succeeding repetitions, and the progression of the mean values of the dynamic coefficient of friction as shown in Fig. 8b. Fellers *et al.* (1998) and Huttel *et al.* (2014) described similar results for friction measurements with paper against paper and paper against metal. All of the subsequent test series for the friction measurement were performed with paperboard samples cut out in cross-machine direction. Both test series with paperboard samples out of CD were performed with different sliding distances and showed the same increasing tendency of the dynamic coefficient of friction after 100 succeeding repetitions due to the triboelectric charging described in Lenske *et al.* (2017). Furthermore, both test series converged to a constant charging state after several repetitions and remained there for the rest of the test series. In contrast, the peak of the coefficient of friction curve for 55 mm sliding distance was higher than the peak of the curve for the lower sliding distance. At the beginning of the friction test both dynamic coefficients of friction showed the same curve progression. After that, the curve of the coefficient of friction for 30 mm sliding distance declined rapidly due to the end of the measurement distance, while the curve of the coefficient of friction for the higher sliding distance increased further. Due to those characteristic curve progressions, the triboelectric charging of the contact area must have been affected by the sliding distance, building up charge over distance. Elsdon and Mitchell (1976) used a turntable and a loaded sample to measure the dependence of charge transferred to the contact sphere over the circumferential length in relation to the contact time. Elsdon and Mitchell (1976) observed that with increasing time of contact, the charge per unit with a circumferential length of 3 increases until a constant state is reached. To simulate the time under contact for the deep drawing process, all test series for the friction measurement were performed with a sliding distance of 55 mm and 20 mm/s relative velocity.

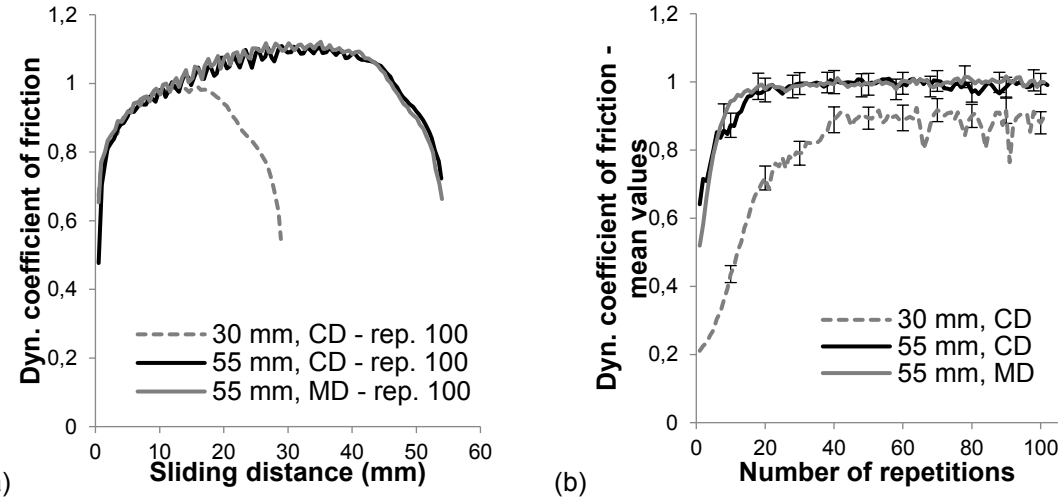

Fig. 8. a) Influence of sliding distance and fiber direction on the progression of the dynamic coefficient of friction after 100 repetitions; b) corresponding progression rates of the mean values for the dynamic coefficient of friction for 100 repetitions (800 N; 20 mm/s; and 23 °C)

The effect of four different normal forces on the dynamic coefficient of friction is shown in Fig. 9 for unheated tools at 23 °C and 20 mm/s relative velocity. Generally, all four curves of the dynamic coefficient of friction representing the four test series after 100 succeeding repetitions had nearly the same progression, but noticeably different peaks. With increased normal force, the dynamic coefficient of friction increased too and it remained constant after reaching a certain charging state, as it was assumed in Lenske *et al.* (2017). Due to the increasing tensile force, the test series with 1200 N normal force stopped after several repetitions due to rupture of the paperboard samples that was similar to the results for the deep drawing process with 500 N constant blank holder force.

The charge transferred due to frictional contact was directly proportional to the real area of contact and therefore proportional to the normal force (Rose and Ward 1957; Elsdon and Mitchell 1976). Huttel *et al.* (2014) describes similar results for normal forces in the range from 100 N to 750 N. After that there is a constant progression of the coefficient of friction with increasing normal force (Huttel *et al.* 2014). However, the dynamic coefficients of friction (Fig. 7) during the deep drawing process seemed noticeably lower than the coefficients of friction for the corresponding normal forces during the double strip testing method. The deep drawing process with the high blank holder force profile ended after 32 repetitions due to rupture of the following repetitions shortly before the paperboard left the contact between blank holder and forming cavity. In contrast, without the influence of the wrinkle formation, the corresponding friction measurement was performed for 100 repetitions and reached a constant charging state without failure. In theory, by reducing the dynamic coefficient of friction between blank holder and top side of the forming cavity, by an appropriate coating, the dynamic coefficient of friction within the forming gap could likely reach the same value for the corresponding friction measurement test series. This approach should be considered for further testing creating a customized friction design for the deep drawing process. In contrast to this, the test series with the low blank holder force profile failed due to rupture within the forming gap, even when the friction measurement test fails after a couple of repetitions without the influence of the wrinkle formation.

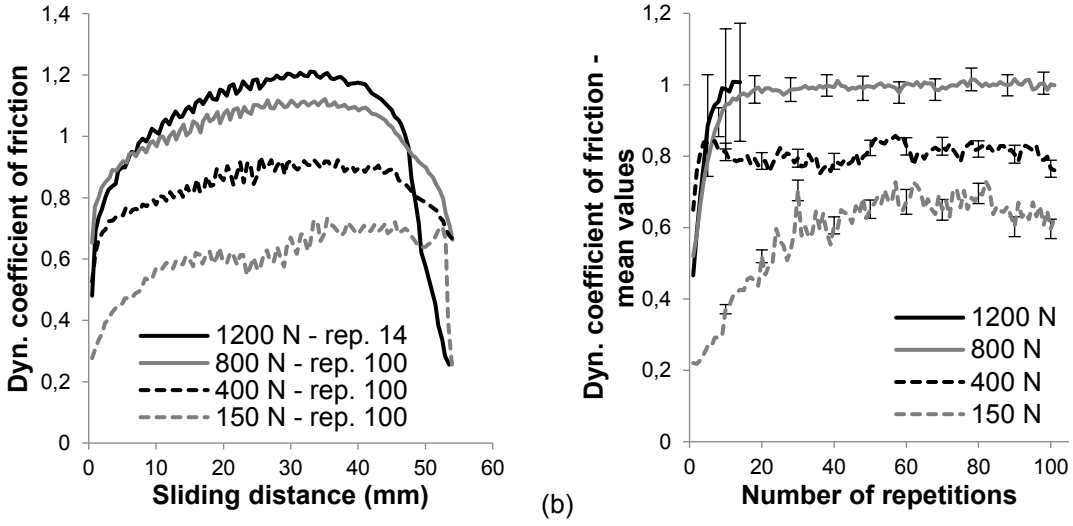

Fig. 9. a) Influence of normal force on the progression of the dynamic coefficient of friction for unheated tools, b) corresponding progression rates of the mean values for the dynamic coefficient of friction for 100 repetitions (20 mm/s; 23 °C)

Figure 10 shows the influence of different normal forces on the dynamic coefficient of friction with heated tools at 60 °C and 20 mm/s relative velocity. Generally, all five test series reached a constant state after 100 succeeding repetitions, but the general progression of the dynamic coefficient of friction was highly force dependent. Up to 400 N constant normal load the dynamic coefficient of friction for one repetition is fairly even without a peak point (Lenske *et al.* 2017). In contrast, with further increased normal force the dynamic coefficient of friction increased noticeably. Furthermore, the progression of the curves developed a peak point roughly 10 mm before the end of the friction measurement. Back (1991) shows similar results for three different paperboards and temperature levels. The dynamic coefficient of friction in Back (1991) for 60 °C is higher than with 120 °C. Unfortunately, Back (1991) did not give information about the normal force that was used for the friction tests. Therefore, Huttel and Post (2015) found that the coefficient of friction increases with increasing normal pressure with heated tools at 90 °C. They assumed that the water in the paperboard sample vaporizes and acts as a type of lubricant. Huttel and Post (2015) speculated that with increasing normal pressure, more water is forced out of the paperboard and therefore the coefficient of friction increases, too. In contrast, Zhang *et al.* (2015) states that the charge carriers are most likely ions dissolved in water, and adsorbed on the insulator surface. With 60 °C contact temperature, the surface layers of the water on the paperboard evaporated, which led to a slightly increasing progression curve of the coefficient of friction. With the increased normal pressure, which probably forced the water from the inside of the paperboard to the surface, enough charge carriers were available for the increased tribocharging. The maintenance of the build-up tribocharging could be correlated with the general higher evaporation heat of metal surfaces. Further testing should be done that searches for a critical normal pressure in comparison to the contact temperature.

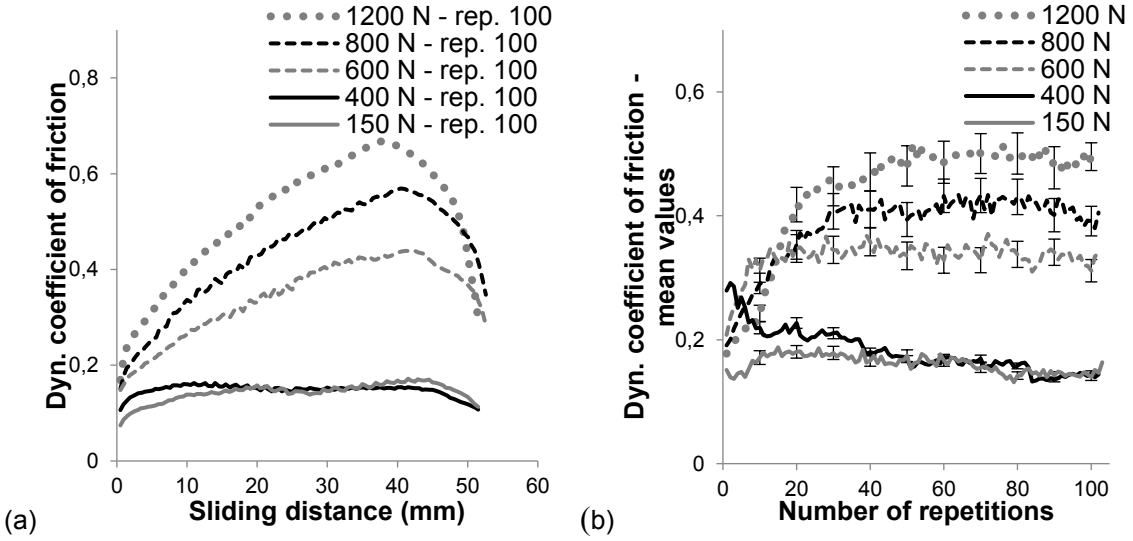

Fig. 10. Influence of normal force on the progression of the dynamic coefficient of friction for heated tools at 60 °C, corresponding progression rates of the mean values for the dynamic coefficient of friction for 100 repetitions

Both deep drawing test series with heated tools at 60 °C in Fig. 7 exhibited an equal progression of the dynamic coefficient of friction for one repetition. The deep drawing test series with low blank holder force profile could be compared with the results in Fig. 9. On

the other hand, the coefficient of friction, which was measured with the strip testing method, was noticeably lower than the corresponding coefficient of friction for the deep drawing test with the high blank holder force profile. During the deep drawing process, the material excess accumulated within the characteristic wrinkles. Müller *et al.* (2017b) concluded that a high blank holder force induces a fine and evenly distributed wrinkle arrangement. Because of this effect, the contacting surface area of the paperboard with the tool surfaces must decrease and, therefore the amount of surface water that could evaporate during the deep drawing process must decrease too. With a fine and evenly distributed wrinkle arrangement, the in-plane pressure within the paperboard must also increase. Thus, a lower amount of normal pressure was needed to force water from the inside of the paperboard to the outside and therefore could function as charge carrier. To establish the accuracy of the results depicted in Fig. 10, Fig. 11 shows the difference between the first and the last repetition of the deep drawing test series for heated tools at 60 °C. The triboelectric charging due to frictional contact increased at first after 20 mm to 25 mm punch movement, shortly before the paperboard left the contact of the blankholder. Beforehand, only a slightly increase of the punch force could be measured, which meant that there was no triboelectric charging. This can be compared to the results in Lenske *et al.* (2017) for heated tools at 60 °C and 0.3 MPa normal pressure. With no or only a slightly increasing wrinkle formation under the blankholder, the results of the deep drawing process and the strip-testing method can be compared with each other. Afterwards, the full wrinkle formation within the forming gap must affect the dynamic coefficient of friction. Further testing should consider the wrinkle formation as an influence of the dynamic coefficient of friction.

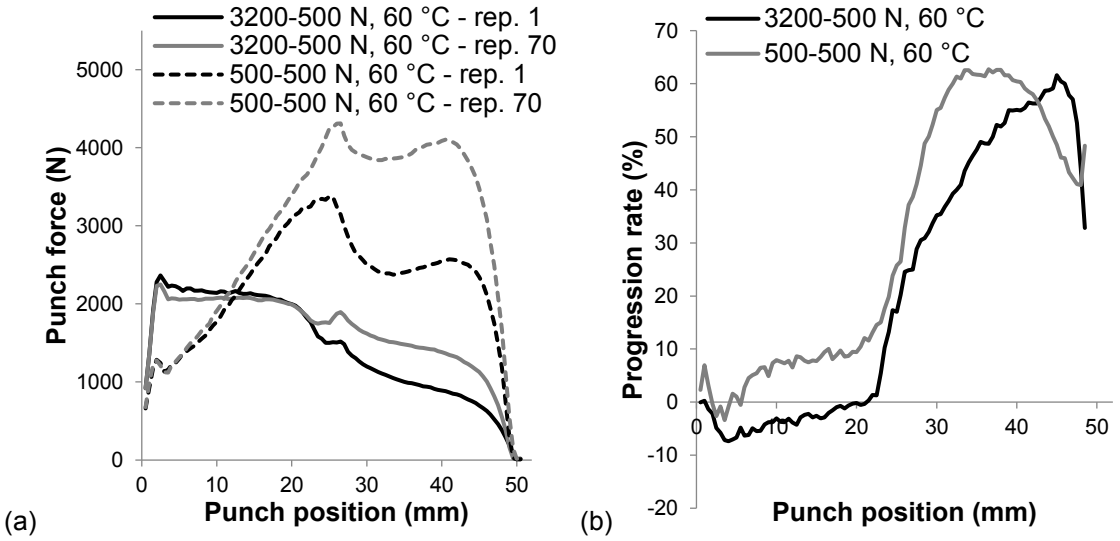

Fig. 11. a) Punch force profiles for the first and the last repetition of the deep drawing test series for heated tools at 60 °C and b) the progression rate between both repetitions

Figure 12 shows the influence of the different normal forces on the dynamic coefficient of friction with heated tools at 120 °C. There was no significant difference between the normal forces in relation to the dynamic coefficient of friction after 100 succeeding repetitions. Similar to the results found in Back (1991) and Vishtal *et al.* (2013), the dynamic coefficients of friction were noticeably lower than the results with unheated tools and heated tools at 60 °C. Furthermore, after reaching a certain charging state the

progression of the mean values of all dynamic coefficients of friction remained constant. Shaw (1917) found that most solids alter their place in the triboelectric series above a certain critical temperature, which is specific for each material. Shaw describes the surface in its new conditions as abnormal. The behavior of the dynamic coefficient of friction during the strip testing method could be compared with the results during the deep drawing process in Fig. 7.

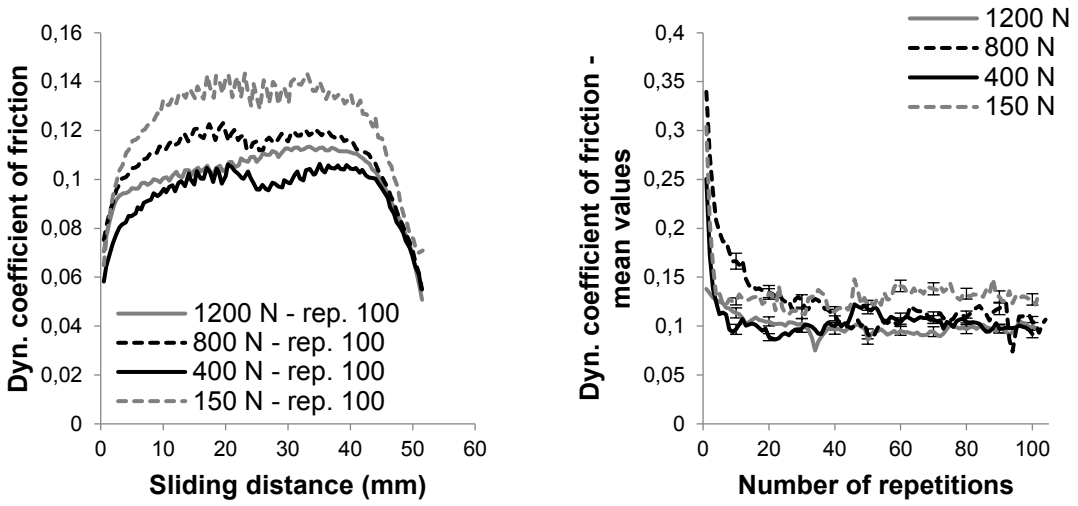

(a) (b)

Fig. 12. a) Influence of normal force on the progression of the dynamic coefficient of friction for heated tools at 120 °C, and b) corresponding progression rates of the mean values for the dynamic coefficient of friction for 100 repetitions

CONCLUSIONS

1. A low blank holder force profile induced a higher gap force than a high blank holder force profile independent of the tool temperature due to the influence of the resulting wrinkle arrangement. With increasing contact temperature, the gap force decreased when using the same blank holder force profile.
2. For unheated tools at 23 °C the fiber direction had a noticeably influence on the compression force within the forming gap. In the machine direction (MD), a higher gap force was measured than in the cross direction (CD). With increasing tool temperature, this influence disappeared completely, except for the test series with low blankholder force profile and 120 °C tool temperature, where in the CD a higher gap force was measured than in the MD.
3. The major influence on the dynamic coefficient of friction between paperboard and metal was the tribocharging of the surfaces in contact due to sliding friction, equal to the results for the deep drawing process.
4. When using the same sample size and the same normal force the sliding distance influenced the dynamic coefficient of friction, reaching a higher tribocharging of the contacting surfaces with higher sliding distance.

5. The fiber direction had no influence on the dynamic coefficient of friction during the friction measurement.
6. The dynamic coefficient of friction increased with increasing normal force and unheated tools at 23 °C. After reaching a certain charging state after several repetitions for the same normal force, the dynamic coefficient of friction remained constant. The test series with 1200 N normal force ended after only a couple of repetitions due to rupture.
7. The dynamic coefficient of friction decreased with increasing contact temperature for 60 °C and 120 °C in relation to the results with unheated tools. For 60 °C, the dynamic coefficient of friction is independent of the normal force until a critical normal force was applied. Afterwards, the dynamic coefficient of friction increased with increasing normal force. In contrast, the dynamic coefficient of friction for 120 °C was independent of the applied normal force.
8. The full wrinkle formation within the forming gap affected the dynamic coefficient of friction for the test series with unheated tools and heated tools at 60 °C. The behavior of the dynamic coefficient of friction for the deep drawing process and the double-strip testing method for heated tools at 120 °C was equal.

ACKNOWLEDGMENTS

The authors would like to thank the German Federation of Industrial Research Associations for their funding (Project No. 18047N). Furthermore, gratitude is also directed to Coesfeld Materialtest GmbH & Co. KG for their technical support developing the friction tester. The authors acknowledge Stefan Büttner from the Chair of Processing Machines and Mobile Machines of the TU Dresden for his software support. The authors acknowledge support by the German Research Foundation and the Open Access Publication Funds of the TU Dresden.

REFERENCES CITED

Back, E. (1991). "Paper-to-paper and paper-to-metal friction," in: *TAPPI International Paper Physics Conference*, Kona, HI, USA, pp. 49-65.

Burgo, T. A. L., Silva, C. A., Balestrin, L. B. S., and Galembeck, F. (2013). "Friction coefficient dependence on electrostatic tribocharging," *Scientific Reports* 3, 1-8, Article ID 2384. DOI: 10.1038/srep02384

DIN EN ISO 1924-2 (2009). "Paper and board – Determination of tensile properties – Part 2: Constant rate of elongation method (20 mm/s)," German Institute for Standardization, Berlin, Germany.

DIN EN 10027-2 (2015). "Designation systems for steels – Part 2: Numerical system," German Institute for Standardization, Berlin, Germany

Elsdon, R., and Mitchell, F. R. G. (1976). "Contact electrification of polymers," *Journal of Physics D- Applied Physics* 9(10), 1445-1460. DOI: 10.1088/0022-3727/9/10/010

EN ISO 287 (2009). "Paper and board – Determination of moisture content of a lot – Oven drying method," European Committee for Standardization, Brüssels, Belgium.

Fellers, C., Backstrom, M., Htun, M., and Lindholm, G. (1998). "Paper-to-paper friction – Paper structure and moisture," *Nordic Pulp and Paper Research Journal* 13(3), 227-232.

Hauptmann, M. (2010). *Die Gezielte Prozessführung und Möglichkeiten zur Prozessüberwachung Beim Mehrdimensionalen Umformen von Karton Durch Ziehen* [*Process Control and Process Monitoring Options in Multidimensional Forming of Cartonboard Through Drawing*], Ph.D. Dissertation, Technische Universität Dresden, Dresden, Germany.

Hauptmann, M. (2017). "*Neue Einsatzpotentiale Naturfaserbasierter Materialien in der Konsumgüterproduktion Durch die Technologische Entwicklung des Ziehverfahrens am Beispiel der Verpackung* [*New Application Potential of Natural Fiber-based Materials in Consumer Goods Production Through the Technological Development of the Deep Drawing Process of Paperboard Using the Example of Packaging*]," Ph.D. Habilitationsschrift, Technische Universität Dresden, Dresden, Germany.

Hauptmann, M., and Majschak, J. P. (2011). "New quality level of packaging components from paperboard through technology improvement in 3D forming," *Packaging Technology and Science* 24(7), 419-432. DOI: 10.1002/pts.941

Hauptmann, M., Wallmeier, M., Erhard, K., Zelm, R., and Majschak, J. P. (2015). "The role of material composition, fiber properties, and deformation mechanisms in the deep drawing of paperboard," *Cellulose* 22(5), 3377-3395. DOI: 10.1007/s10570-015-0732-x

Hauptmann, M., Weyhe, J., and Majschak, J. P. (2016). "Optimisation of deep drawn paperboard structures by adaption of the blank holder force trajectory," *Journal of Materials Processing Technology* 232, 142-152. DOI: 10.1016/j.jmatprotec.2016.02.007

Huttel, D., Groche, P., May, A., and Euler, M. (2014). "Friction measurement device for fiber material forming processes," *Advanced Materials Research* 966-967, 65-79. DOI: 10.4028/www.scientific.net/AMR.966-967.65

Huttel, D., and Post, P.-P. (2015). *Anwendung wirkmedienbasierter Verfahren zum Tiefziehen von Papier und Karton* (IGF 17788N) [*Application of Media-based Methods for Deep-drawing of Paper and Cardboard (IGF* 17788N)], German Federation of Industrial Research Association (AiF), Darmstadt, Germany.

Lenske, A., Müller, T., Hauptmann, M., and Majschak, J. P. (2017). "Evaluating the factors influencing the friction behavior of paperboard during the deep drawing process," *BioResources* 12(4), 8340-8358. DOI: 10.15376/biores.12.4.8340-8358

Lowell, J. (1988). "Contact charging: The effect of sample history," *Journal of Physics D- Applied Physics* 21, 138-147. DOI: 10.1088/0022-3727/21/1/019

Müller, T., Lenske, A., Hauptmann, M., and Majschak, J. P. (2017a). "Method for fast quality evaluation of deep-drawn paperboard packaging components," *Packaging Technology and Science* 30(11), 703-710. DOI: 10.1002/pts.2315

Müller, T., Lenske, A., Hauptmann, M., and Majschak, J.-P. (2017b). "Analysis of dominant process parameters in deep-drawing of paperboard," *BioResources* 12(2), 3530-3545. DOI: 10.15376/biores.12.2.3530-3545

Niskanen, K. (1998). *Paper Physics*, Papermaking Science and Technology series, No. 16, Fapet Oy, Helsinki.

Rose, G. S., and Ward, S. G. (1957). "Contact electrification across metal-dielectric and dielectric-dielectric interfaces," *British Journal of Applied Physics* 8(1957), 121-126.

Scherer, K. (1932). *Untersuchungen über die Ziehfähigkeit und den Ziehvorgang von Pappe* [*Investigation on the Drawing Ability and the Drawing of Cardboard*], Ph.D. Dissertation, Sächsische Technische Hochschule zu Dresden [Saxonian Technical University Dresden], Dresden, Germany.

Shaw, P. E. (1917). "Experiments on tribo-electricity- The tribo-electric series," *Proceedings of the Royal Society* 94(656), 16-33. DOI: 10.1098/rspa.1917.0046

Steenberg, B. (1947). "Paper as a visco-elastic body," *Svensk Papperstidning* 50(69), 127-140.

Tanninen, P., Matthews, S., Ovaska, S. S., Varis, J., and Backfolk, K. (2017). "A novel technique for the evaluation of paperboard performance in press-forming," *Journal of Materials Processing Technology* 240, 284-292. DOI: 10.1016/j.jmatprotec.2016.10.002

Tenzer, H. J. (1989). *Leitfaden der Papierverarbeitungstechnik* [*Guide to Paper Processing*], Verlag für Fach- und Bibliothekswesen [Publisher for specialized and librarianship], Leipzig, Germany.

Vishtal, A., Hauptmann, M., Zelm, R., Majschak, J. P., and Retulainen, E. (2013). "3D forming of paperboard: The influence of paperboard properties of formability," *Packaging Technology and Science* 27(9), 677-691. DOI: 10.1002/pts.2056

Zhang, Y., Pähtz, T., Liu, Y., Wang, X., Zhang, R., Shen, Y., Ji, R., and Cai, B. (2015). "Electric field and humidity trigger contact electrification," *Physical Review X* 5(1), 1-9, Article ID 011002. DOI: 10.1103/PhysRevX.5.011002

Article submitted: February 22, 2018; Peer review completed: May 19 2018; Revised version received and accepted: May 23, 2018; Published: